Average Error Rate Analysis for Pilot-aided OFDM Receivers with Frequency-domain Interpolation

Yasamin Mostofi
Department of Electrical Engineering
Stanford University
Stanford, CA 94305, USA
Email: yasi@wireless.stanford.edu

Donald C. Cox
Department of Electrical Engineering
Stanford University
Stanford, CA 94305, USA
Email: dcox@spark.stanford.edu

***Abstract*— In OFDM receivers, pilot tones should be inserted among the sub-carriers in order to estimate the channel in high delay spread environments. To estimate the channel at all the sub-carriers, using the pilot tones, different frequency-domain interpolators can be used. For a given number of pilot tones, these interpolators will have different levels of complexity depending on the number of adjacent pilot tones that they use to estimate the channel at each sub-carrier. For high delay-spread channels, as the number of adjacent pilot tones used by an interpolator increases, channel estimation improves resulting in a tradeoff between performance and complexity. In this paper, we first find an analytical average error rate formula for a pilot-aided OFDM receiver in a delay spread fading environment. This analysis will provide a framework to evaluate the performance of different interpolators. As an example, we then evaluate and compare the performance of two interpolators with different levels of complexity: a trigonometric interpolator and a linear one. We derive the average error rate formulas of the interpolators and confirm that the former one has a considerably better performance as the delay spread increases. However, for flat fading channels, we show that the linear interpolator has a 3dB gain. Finally, our simulation results support the mathematical analysis and comparison.**

I. Introduction

Orthogonal Frequency Division Multiplexing (OFDM) handles delay spread by sending low data rates at all the sub-channels in parallel [1]-[2]. By adding a guard interval to the beginning of each OFDM symbol, the effect of delay spread (provided that there is perfect synchronization) would appear as a multiplication in the frequency domain for a time-invariant channel. Adding the guard interval will also prevent Inter-OFDM Symbol-Interference. In high delay spread environments, in order to estimate and remove the effect of channel coefficients in the frequency domain, pilot tones should be transmitted. The minimum number of pilot tones required in each OFDM symbol exceeds normalized channel delay by one where normalized channel delay refers to the channel delay divided by the sampling period. These pilot tones should be equally spaced in the frequency domain to minimize noise enhancement. To estimate the channel in the sub-bands in between the pilot tones, different interpolators with different levels of complexity can be used.

In this paper, we first find a general formula for the average error rate of an OFDM system in the presence of channel estimation error. Authors in [3] found a formula for the error rate in the case that pilot tones have been inserted in all the sub-carriers. Therefore, the effect of interpolation was not studied in their work. Furthermore, their work can not be extended to address interpolation since they made a limiting assumption that the channel estimation error is independent of the value of the channel at each sub-carrier, which may not be the case depending on the interpolator. In this paper we take a different approach, which enables us to find the average error rate of a pilot-aided OFDM system analytically without a need to make this assumption. Then we evaluate the error rate of two specific interpolators. The first one is based on an IFFT, zero padding and an FFT operation. The second interpolator is a linear one. A complete mathematical analysis is provided for both interpolators, which allows for a comparison of the two. Finally, our simulation results support the analysis.

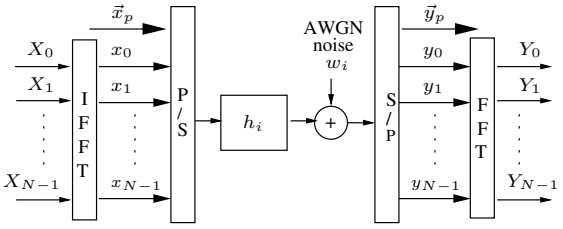

Fig. 1 Discrete baseband equivalent model

II. System Model

Fig. 1 shows the discrete baseband equivalent system model. The available bandwidth is divided into N sub-channels and the guard interval spans G sampling periods. We assume that the normalized length of the channel is always less than or equal to G in this paper. X_i represents the transmitted data in the i^{th} frequency sub-band and is related to the time domain sequence, x_i, as follows:

$$X_i = \sum_{k=0}^{N-1} x_k e^{-\frac{j2\pi ki}{N}} \quad 0 \le i \le N-1 \tag{1}$$

$\vec{x}_p$ is the cyclic prefix vector with length G, h_i represents the i^{th} channel tap with Rayleigh fading amplitude and uniformly

distributed phase and w_i is AWGN noise. After the FFT operation in the receiver, at the i^{th} sub-channel, we will have,

$$Y_i = H_i X_i + W_i \quad 0 \le i \le N-1 \tag{2}$$

where $H_i = \sum_{k=0}^{N-1} h_k e^{-\frac{j2\pi ki}{N}}$ denotes the channel and W_i, the FFT of w_i, is the noise in the i^{th} sub-carrier.

III. Average error rate analysis

Let $H_i = \alpha_i e^{j\theta_i}$ and $\hat{H}_i = \hat{\alpha}_i e^{j\hat{\theta}_i}$ where α_i and $\hat{\alpha}_i$ are Rayleigh fading amplitudes and θ_i and $\hat{\theta}_i$ are uniformly distributed phases. $\hat{H}_i$ is the estimated channel at the i^{th} sub-carrier. To estimate the transmitted data from Eq. 2, we will have,

$$\hat{X}_i = \frac{\alpha_i}{\hat{\alpha}_i} e^{j\phi_i} X_i + \frac{U_i}{\hat{\alpha}_i} \tag{3}$$

where $\phi_i = \theta_i - \hat{\theta}_i$ and $U_i = U_R(i) + jU_I(i) = W_i e^{-j\hat{\theta}_i}$ is a Gaussian noise with the same characteristics as W_i. In this paper, we assume that X_i is a 4PSK modulated signal with power of σ_X^2. Extending the analysis to other modulations should be a straight forward extension of the work done in this paper. For one realization of ϕ_i and α_i, the instantaneous probability of receiving the correct symbol of the constellation at the i^{th} sub-carrier will be,

$$P_{c,inst.}(i) = Prob\{\frac{\sigma_X \alpha_i (cos\phi_i - sin\phi_i)}{\sqrt{2}\hat{\alpha}_i} + \frac{U_R(i)}{\hat{\alpha}_i} > 0 \quad \& \quad \frac{\sigma_X \alpha_i (cos\phi_i + sin\phi_i)}{\sqrt{2}\hat{\alpha}_i} + \frac{U_I(i)}{\hat{\alpha}_i} > 0\} \tag{4}$$

where $U_R(i)$ and $U_I(i)$ are uncorrelated and have Gaussian distributions (hence they are independent) with zero means and variances of $\sigma_{U_R}^2 = \sigma_{U_I}^2 = .5\sigma_U^2$, where $\sigma_U^2 = \overline{|U_i^2|} = \overline{|W_i^2|}$. Then, $P_{c,inst.}$ will be as follows:

$$P_{c,inst.}(i) = Q(\frac{-\sigma_X \alpha_i (cos\phi_i - sin\phi_i)}{\sigma_U}) \times Q(\frac{-\sigma_X \alpha_i (cos\phi_i + sin\phi_i)}{\sigma_U})$$

$$\Rightarrow P_{e,inst.}(i) = 1 - P_{c,inst.}(i) = \tag{5}$$

$$Q(\frac{\sigma_X \alpha_i (cos\phi_i - sin\phi_i)}{\sigma_U}) + Q(\frac{\sigma_X \alpha_i (cos\phi_i + sin\phi_i)}{\sigma_U}) - Q(\frac{\sigma_X \alpha_i (cos\phi_i - sin\phi_i)}{\sigma_U}) \times Q(\frac{\sigma_X \alpha_i (cos\phi_i + sin\phi_i)}{\sigma_U})$$

where $Q(s) = \frac{1}{\sqrt{2\pi}} \int_s^\infty e^{-\frac{z^2}{2}} dz$ for an arbitrary s. To evaluate the average error rate, $\overline{P_e}$, $P_{e,inst.}$ should be averaged over the distributions of α_i and ϕ_i. First we perform an averaging over α_i, which has a Rayleigh distribution. Since the last term of Eq. 5 has a considerably smaller value than other terms (as long as the error rate is not too high), we approximate $P_{e,inst.}$ with the first two terms to make the averaging possible. $\overline{P_e}$ evaluated through this approximation is slightly more than the exact one at very high error rates but matches well with it otherwise. It can be shown that for an arbitrary s,

$$\overline{Q(\alpha_i s)} = \frac{2}{\overline{\alpha_i^2}} \int_0^\infty Q(\alpha_i s) \alpha_i e^{-\frac{\alpha_i^2}{\overline{\alpha_i^2}}} d\alpha_i$$

$$= \frac{1}{2} - \frac{s}{\sqrt{2\pi}} \int_0^\infty e^{-\frac{\alpha_i^2}{2}(s^2 + \frac{2}{\overline{\alpha_i^2}})} d\alpha_i = \frac{1}{2} \times (1 - \frac{s}{\sqrt{s^2 + \frac{2}{\Omega_i}}}) \tag{6}$$

where,

$$\Omega_i = \overline{\alpha_i^2} = \overline{H_i H_i^*} = \sum_m \sum_n \overline{h_m h_n^*} e^{-\frac{j2\pi i(m-n)}{N}} \tag{7}$$

Since $\overline{h_m h_n^*} = \sigma_{h_m}^2 \delta_{m,n}$, where $\sigma_{h_m}^2 = \overline{|h_m|^2}$, we will have,

$$\Omega_i = \sum_m \sigma_{h_m}^2 \tag{8}$$

We drop the index i of Ω_i since it is not a function of i: $\Omega = \sum_m \sigma_{h_m}^2$. Using Eq. 5-8, the average error rate will be as follows,

$$\overline{P_e}(i) = 1 - .5\sqrt{\frac{SNR_{rec}}{2}} \times E_{\phi_i} \left\{ \frac{cos(\phi_i) - sin(\phi_i)}{\sqrt{1 + \frac{SNR_{rec}(1 - sin(2\phi_i))}{2}}} \right\} - .5\sqrt{\frac{SNR_{rec}}{2}} \times E_{\phi_i} \left\{ \frac{cos(\phi_i) + sin(\phi_i)}{\sqrt{1 + \frac{SNR_{rec}(1 + sin(2\phi_i))}{2}}} \right\} \tag{9}$$

where SNR_{rec}, the average received Signal to Noise Ratio, is defined as $SNR_{rec} = \frac{\Omega \sigma_X^2}{\sigma_U^2}$ and $E_{z_1}\{z_2\}$ represents average of z_2 with respect to z_1 for arbitrary z_1 and z_2. The distribution of ϕ_i is as follows [4]:

$$p(\phi_i) = \left[\frac{\sqrt{1 - \rho_i cos^2(\phi_i)} + \sqrt{\rho_i} cos(\phi_i)(\pi - cos^{-1}(\sqrt{\rho_i} cos(\phi_i)))}{(1 - \rho_i cos^2(\phi_i))^{1.5}} \right] \times \frac{(1 - \rho_i) \times (2\pi - |\phi_i|)}{4\pi^2} \quad |\phi_i| \le 2\pi \tag{10}$$

where $\rho_i = \frac{cov(\alpha_i^2, \hat{\alpha}_i^2)}{\sqrt{var(\alpha_i^2) var(\hat{\alpha}_i^2)}}$ with $cov(\alpha_i^2, \hat{\alpha}_i^2) = \overline{\alpha_i^2 \hat{\alpha}_i^2} - \overline{\alpha_i^2} \times \overline{\hat{\alpha}_i^2}$ and $var(\alpha_i^2) = \overline{\alpha_i^4} - (\overline{\alpha_i^2})^2$. Then, we will have,

$$\overline{P_e}(i) = 1 - .5\sqrt{\frac{SNR_{rec}}{2}} \int_{\phi_i} \frac{cos(\phi_i) - sin(\phi_i)}{\sqrt{1 + \frac{SNR_{rec}(1 - sin(2\phi_i))}{2}}} \times p(\phi_i) d\phi_i - .5\sqrt{\frac{SNR_{rec}}{2}} \int_{\phi_i} \frac{cos(\phi_i + sin(\phi_i)}{\sqrt{1 + \frac{SNR_{rec}(1 + sin(2\phi_i))}{2}}} \times p(\phi_i) d\phi_i \tag{11}$$

$\overline{P_e}(i)$ of Eq. 11 is a function of i through ρ_i.

IV. Pilot-aided channel estimation

Let $\nu \le G$ be the maximum predicted normalized length of the channel. It can be shown that only $L = \nu + 1$ equally spaced pilot tones are required for channel estimation [5]. Therefore, we insert $L = \nu + 1$ equally spaced pilots, $X_{pilot}(l_i)$, at sub-channels $l_i = \frac{i \times N}{L}$ for $0 \le i \le L-1$. An estimate of the channel at pilot tones can then be acquired as follows:

$$\hat{H}_{l_i} = \frac{Y_{l_i}}{X_{pilot}(l_i)} = H_{l_i} + \frac{W_{l_i}}{X_{pilot}(l_i)} \quad 0 \le i \le L-1 \tag{12}$$

To estimate the channel at sub-carriers in between the pilot tones, different interpolators can be used. The complexity of these interpolators varies depending on the number of pilot tones used to estimate the channel at each sub-carrier. In this paper we analyze two extreme cases. The first interpolator uses all the pilots to estimate the channel at each sub-band. The second one, on the other hand, only uses the two adjacent pilot tones. Therefore the former one will have a superior performance in environments with considerable delay spread at the cost of an increase in the complexity.

A. A Trigonometric Interpolator

To find the time domain channel from Eq. 12, an IFFT of length L should be performed. The time-domain channel estimate, $\hat{h}_k$, would be as follows,

$$\hat{h}_k = \frac{1}{L}\sum_{i=0}^{L-1} \hat{H}_{l_i} e^{\frac{j2\pi ik}{L}} \quad 0 \le k \le L-1 \tag{13}$$

Through an FFT of length N, the estimate of the channel at all the sub-carriers will be as follows:

$$\hat{H}_i = \sum_{k=0}^{L-1} \hat{h}_k e^{\frac{-j2\pi ik}{N}} \quad 0 \le i \le N-1 \tag{14}$$

It is also possible to find $\hat{H}_i$ directly from the pilots without a need to go to the time domain. Using Eq. 13 and 14, we will have,

$$\begin{aligned} &\hat{H}_i = \\ &\tfrac{1}{L}\textstyle\sum_{m=0}^{L-1}\sum_{k=0}^{L-1} \hat{H}_{l_m} e^{-j2\pi k(\frac{i}{N}-\frac{m}{L})} \quad 0 \le i \le N-1 \\ &= \tfrac{1}{L}\textstyle\sum_{m=0}^{L-1} \hat{H}_{l_m} \frac{1-e^{-\frac{j2\pi i}{r}}}{1-e^{-j2\pi(\frac{i}{N}-\frac{m}{L})}} \\ &= \textstyle\sum_{m=0}^{L-1} \underbrace{\frac{1-e^{-\frac{j2\pi i}{r}}}{2Lj}(cot(\frac{\pi i}{N}-\frac{\pi m}{L})+j)}_{\beta_{i,m}} \times \hat{H}_{l_m} \end{aligned} \tag{15}$$

where $r = \frac{N}{L}$ and $cot(s) = \frac{cos(s)}{sin(s)}$ for an arbitrary s. From Eq. 15, it can be seen that to estimate the channel at any sub-carrier, all the L pilots have been used. We refer to this interpolator as a "trigonometric interpolator" since the coefficient of $\hat{H}_{l_m}$ is a trigonometric function of i in Eq. 15. Inserting Eq. 12 in Eq. 15, we will have,

$$\hat{H}_i = H_i + \sum_{m=0}^{L-1} \beta_{i,m} \frac{W_{l_m}}{X_{pilot}(l_m)} \tag{16}$$

From Eq. 16, we can find ρ_i for this interpolator. We will have,

$$\hat{\Omega}_{i,A} = \overline{\hat{\alpha}_i^2} = \overline{|\hat{H}_i|^2} = \Omega + \frac{\sigma_U^2}{\sigma_X^2}\sum_{m=0}^{L-1} |\beta_{i,m}^2| \quad 0 \le i \le N-1 \tag{17}$$

The subscript A in $\hat{\Omega}_{i,A}$ refers to the trigonometric interpolator. It can be easily proven that $\sum_{m=0}^{L-1} |\beta_{i,m}^2| = 1$ for any i. Therefore, we will have,

$$\hat{\Omega}_{i,A} = \Omega + \frac{\sigma_U^2}{\sigma_X^2} \quad 0 \le i \le N-1 \tag{18}$$

We drop the index i of $\hat{\Omega}_{i,A}$ since it is not a function of it as can be seen from Eq. 18. It is easy to show that $\overline{s^4} = 2(\overline{s^2})^2$ and hence $var(s^2) = (\overline{s^2})^2$ for a Rayleigh distributed variable s. Thus, $var(\alpha_i^2) = \Omega^2$ and $var(\hat{\alpha}_i^2) = \hat{\Omega}_A^2$. Using these equalities, we calculate $\overline{\alpha_i^2\hat{\alpha}_i^2}$ as follows:

$$\overline{\alpha_i^2\hat{\alpha}_i^2} = \overline{|H_i|^2|\hat{H}_i|^2} = 2\Omega^2 + \frac{\sigma_U^2}{\sigma_X^2}\Omega \tag{19}$$

Finally, ρ_i will be as follows for this interpolator,

$$\rho_{i,A} = \frac{\overline{\alpha_i^2\hat{\alpha}_i^2} - \Omega\hat{\Omega}_A}{\Omega\hat{\Omega}_A} = \frac{\Omega}{\hat{\Omega}_A} = \frac{SNR_{rec}}{1+SNR_{rec}} \tag{20}$$

As can be seen, for this interpolator, ρ_i and therefore $\overline{P_i}$ are neither functions of i nor functions of the shape of the channel delay profile and are solely a function of SNR_{rec}.

B. A Linear Interpolator

It is also possible to estimate the channel at all the sub-carriers by a linear interpolation. In this case, at each sub-carrier, the channel is estimated using only the two adjacent pilots. Therefore, This interpolator will be less computationally complex than the one of the previous section. For this interpolator, we will have,

$$\hat{H}_i = \gamma_i\hat{H}_{d_i} + \eta_i\hat{H}_{d_i+r} \quad 0 \le i \le N-1 \tag{21}$$

where $d_i = floor(\frac{i}{r}) \times r$ refers to the sub-carriers with pilot tones, $\eta_i = \frac{i-d_i}{r}$ and $\gamma_i = 1-\eta_i$. Using Eq. 12, we will have,

$$\hat{H}_{d_i} = H_{d_i} + \frac{W_{d_i}}{X_{pilot}(d_i)} \tag{22}$$

Therefore for $0 \le i \le N-1$,

$$\hat{H}_i = \gamma_i H_{d_i} + \gamma_i\frac{W_{d_i}}{X_{pilot}(d_i)} + \eta_i H_{d_i+r} + \eta_i\frac{W_{d_i+r}}{X_{pilot}(d_i+r)} \tag{23}$$

Using Eq. 23, we can find $\hat{\Omega}_{i,B}$ where index B refers to the linear interpolator,

$$\hat{\Omega}_{i,B} = (\gamma_i^2+\eta_i^2)\times(\Omega + \frac{\sigma_U^2}{\sigma_X^2}) + 2\gamma_i\eta_i \times real(R_H(r)) \tag{24}$$

where $R_H(s)$, the auto-correlation function of the wide-sense stationary process H, is defined as $R_H(s) = \overline{H_{s+t}H_t^*} = \sum_m \sigma_{h_m}^2 e^{-\frac{j2\pi ms}{N}}$ and $\Omega = R_H(0)$ is as defined in the previous part. Next, we calculate the covariance. Using Eq. 23, we will have,

$$\begin{aligned} &\overline{\alpha_i^2\hat{\alpha}_i^2} = \overline{H_iH_i^*\hat{H}_i\hat{H}_i^*} = \\ &\gamma_i^2\overline{H_iH_i^*H_{d_i}H_{d_i}^*} + \eta_i^2\overline{H_iH_i^*H_{d_i+r}H_{d_i+r}^*} + \\ &2\gamma_i\eta_i \times real(\overline{H_iH_i^*H_{d_i}H_{d_i+r}^*}) + (\gamma_i^2+\eta_i^2)\tfrac{\Omega\sigma_U^2}{\sigma_X^2} \end{aligned} \tag{25}$$

To evaluate the terms in Eq. 25, we have to calculate $\overline{H_i H_i^* H_m H_n^*}$ for an arbitrary m and n. We will have,

$$\overline{H_i H_i^* H_m H_n^*} = \sum_k \sum_{k'} \sum_{k''} \sum_{k'''} \overline{h_k h_{k'}^* h_{k''} h_{k'''}^*} e^{-\frac{j2\pi((k-k')i+mk''-nk''')}{N}}$$

$$= \sum_k \overline{|h_k|^4} e^{\frac{-j2\pi k(m-n)}{N}} + \underbrace{\sum_{k=k'} \sum_{k''=k'''}}_{k\neq k''} \sigma_{h_k}^2 \sigma_{h_{k''}}^2 e^{-\frac{j2\pi(m-n)k''}{N}}$$
$$+ \underbrace{\sum_{k=k'''} \sum_{k'=k''}}_{k\neq k'} \sigma_{h_k}^2 \sigma_{h_{k'}}^2 e^{-\frac{j2\pi((k-k')i+mk'-nk)}{N}}$$
$$+ \underbrace{\sum_{k=k''} \sum_{k'=k'''}}_{k\neq k'} \overline{h_k^2 h_{k'}^{*2}} e^{-\frac{j2\pi((k-k')i+mk-nk')}{N}} \quad (26)$$

For an h_k with Rayleigh fading amplitude and uniformly distributed phase, $\overline{h_k^2} = 0$. Therefore, the last term on the right hand side of Eq. 26 is zero. Evaluating the rest of the terms, we will have,

$$\overline{H_i H_i^* H_m H_n^*} = 2R_{4H}(m-n) + \Omega R_H(m-n) - R_{4H}(m-n) + R_H(i-n)R_H(m-i) - R_{4H}(m-n) = \Omega R_H(m-n) + R_H(i-n)R_H(m-i) \quad (27)$$

where $R_{4H}(s) = \sum_k \sigma_{h_k}^4 e^{-\frac{j2\pi ks}{N}}$. Using Eq. 27, Eq. 25 can be rewritten as follows,

$$\overline{\alpha_i^2 \hat{\alpha}_i^2} = 2\gamma_i\eta_i \times real(\Omega R_H(r) + R_H(i-d_i)R_H(d_i+r-i)) + \gamma_i^2(\Omega^2 + |R_H(i-d_i)|^2) + \eta_i^2(\Omega^2 + |R_H(i-d_i-r)|^2) + (\gamma_i^2+\eta_i^2)\frac{\Omega\sigma_U^2}{\sigma_X^2} \quad (28)$$

Using Eq. 24 and 28, we will have,

$$cov(\alpha_i^2, \hat{\alpha}_i^2) = \gamma_i^2|R_H(i-d_i)|^2 + \eta_i^2|R_H(i-d_i-r)|^2 + 2\gamma_i\eta_i \times real(R_H(i-d_i)R_H(d_i+r-i)) \quad (29)$$

$$\rho_{i,B} = \frac{\gamma_i^2|R_H(i-d_i)|^2 + \eta_i^2|R_H(i-d_i-r)|^2}{\Omega \times \hat{\Omega}_{i,B}} + \frac{2\gamma_i\eta_i \times real(R_H(i-d_i)R_H(d_i+r-i))}{\Omega \times \hat{\Omega}_{i,B}} \quad (30)$$

To write Eq. 30 as a function of SNR_{rec}, we normalize the power of the channel paths: $\sigma_{h_{k,norm.}}^2 = \frac{\sigma_{h_k}^2}{\Omega}$. Let $R_{H,norm.}(s) = \sum_k \sigma_{h_{k,norm.}}^2 e^{-\frac{j2\pi ks}{N}}$. Then, we can rewrite Eq. 30 as follows:

$$\rho_{i,B} = \frac{\gamma_i^2|R_{H,norm.}(i-d_i)|^2 + \eta_i^2|R_{H,norm.}(i-d_i-r)|^2}{(\gamma_i^2+\eta_i^2)\times(\frac{SNR_{rec}+1}{SNR_{rec}}) + 2\gamma_i\eta_i \times real(R_{H,norm.}(r))} + \frac{2\gamma_i\eta_i \times real(R_{H,norm.}(i-d_i)R_{H,norm.}(d_i+r-i))}{(\gamma_i^2+\eta_i^2)\times(\frac{SNR_{rec}+1}{SNR_{rec}}) + 2\gamma_i\eta_i \times real(R_{H,norm.}(r))} \quad (31)$$

As can be seen from Eq. 31, ρ_i and therefore $\overline{P_i}$ of the linear interpolator are functions of i. There are $\lfloor \frac{r}{2} \rfloor + 1$ different error rates that each sub-carrier may experience depending on its location. For instance, pilot carrying sub-carriers are those with $\eta_i = 0$. From Eq. 31, it can be seen that for these sub-carriers $\rho_{i,B} = \frac{SNR_{rec}}{1+SNR_{rec}}$ which is the same as $\rho_{i,A}$. In general, there are two factors determining the performance of a linear interpolator: noise and delay spread. As a sub-carrier gets farther from the pilot tones, $R_{H,norm.}$ decreases for non-flat channels. For instance, the sub-carrier in the middle of every two consecutive pilot tones has the least correlation. However, the amount of added noise decreases as well. To see this, take the noisy terms, $\gamma_i \frac{W_{d_i}}{X_{pilot}(d_i)} + \eta_i \frac{W_{d_i+r}}{X_{pilot}(d_i+r)}$, of Eq. 23. It can be easily shown that the power of these terms is minimized for $\gamma_i = \eta_i = .5$, which refers to the sub-carriers in the middle of every two consecutive tones. As the delay spread increases, it becomes the dominant factor. Then, $R_{H,norm.}$ decreases and the linear interpolator will have worse performance than the trigonometric one. However, for nearly-flat fading channels, noise becomes the dominant factor. Then linear interpolator will have a better performance than the trigonometric one. For instance, consider the sub-carriers with $\gamma_i = \eta_i = .5$. Inserting $R_{H,norm.} = 1$ (flat fading) in Eq. 31 for these carriers would result in the following:

$$\gamma_i = \eta_i = .5 \quad \& \quad R_{H,norm.} = 1 \Rightarrow \rho_{i,B} = \frac{2SNR_{rec}}{2SNR_{rec}+1} \quad (32)$$

Comparing Eq. 32 with Eq. 20 shows that the linear interpolator has a 3dB gain in this specific case. This is due to the fact that the trigonometric interpolator uses all the pilots for channel estimation at each sub-carrier, which adds more noise than the linear one that solely uses the adjacent pilots. Despite the superiority of the linear interpolator in the flat fading case, since these interpolators are to be used in delay spread environments, the trigonometric one will outperform the linear interpolator.

V. Analysis and Simulation Results

We find $\overline{P_e}(i)$ of Eq. 11 for two different power-delay profiles using the correlation coefficients of the interpolators. Also, we simulate the whole system for both channels to compare the results of analysis and simulation. The power delay profile of both channels has two taps with relative powers of $\frac{2}{3}$ and $\frac{1}{3}$ respectively. The delay between the two taps is $5\mu s$ for channel I and $26\mu s$ for channel II (in both cases, the channel delay is less than the cyclic prefix). Therefore, the frequency response of channel II is less correlated, i.e. $R_{H,norm.}$ has smaller values since it is the FFT of the power-delay profile with a longer delay. Input modulation is 4PSK, $r = 4$, $N = 892$ and the total bandwidth is $3.9MHz$. Since $r = 4$, there are three sub-carriers in between every two consecutive pilots. Therefore for the linear interpolator, there will be three sets of error rates. Set#1 refers to the pilot sub-carriers. In the OFDM symbols with training, pilots are transmitted on these sub-carriers. However, when considering the error rates at these sub-carrier frequencies, it refers to the subsequent symbols, without training, that use the estimate of the channel from the training symbols. For the remaining sub-carriers, error rate analysis applies to both training and non-training symbols. Set#2 refers to the sub-carriers that are

adjacent to one pilot carrier and set#3 denotes the rest of the sub-carriers. Fig. 2 shows $\overline{P_e}$ of channel I as a function of SNR_{rec}. For this channel, the trigonometric and linear interpolators have very similar performance due to low delay spread. It can be seen that, the error rate of set#1 of the linear interpolator is the same as that of the trigonometric one, as was shown in the previous section. Since the delay spread of this channel is low, at low SNR_{rec}, noise is the dominant factor. Therefore, for set#2 and 3, the performance of the linear interpolator is slightly better than the trigonometric one at low SNR_{rec}, as can be seen. On the other hand, at very high SNR_{rec}, delay spread becomes the dominant factor and the trigonometric interpolator slightly outperforms the linear one at set#2 and 3, as can be seen from Fig. 2. This is more pronounced for set#3 since channel values at those subcarriers are less correlated with those at the pilot carrying ones. Fig. 3 shows the error rates for channel II. The performance of the linear interpolator degrades considerably at set#2 and 3 for this channel due to higher delay spread. However, the performance of the trigonometric interpolator stays independent of the shape of the channel. As can be seen, the result of the mathematical analysis and simulation matches well in both Fig. 2 and 3. At very high $\overline{P_e}$, the result of the analysis is slightly higher than the simulation, which is due to the omission of the last term of Eq. 5.

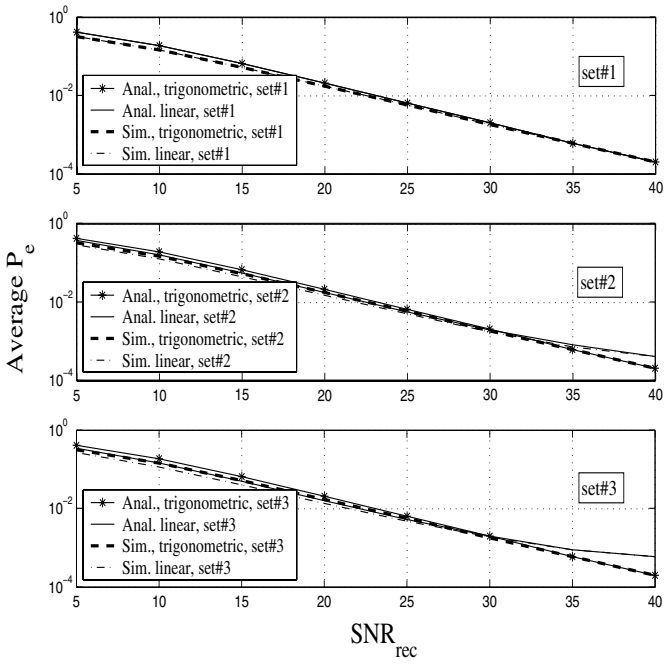

Fig. 2 $\overline{P_e}$ vs. SNR_{rec} for power-delay profile I

VI. Conclusion

In this paper, we derived average probability of error formulas for an OFDM receiver that uses frequency-domain pilot-aided channel estimation. This analysis provided a framework to evaluate the performance of different frequency-domain interpolation methods. As an example, we analyzed the performance of two different interpolators, a trigonometric interpolator and a linear one. We showed mathematically that the average error rate of the former interpolator is independent of the shape of the channel and is solely a function of SNR_{rec}. Furthermore, we showed that as delay spread increases, the performance of the linear interpolator degrades considerably. In the case of a flat fading channel, however, the linear interpolator has a 3dB gain over the trigonometric one due to the smaller contribution of noise sources. Finally, the simulation results confirmed the mathematical analysis.

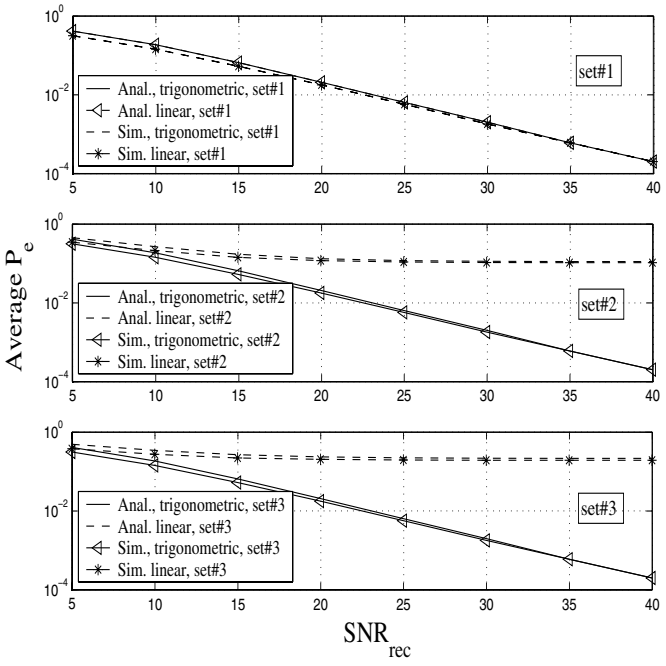

Fig. 3 $\overline{P_e}$ vs. SNR_{rec} for power-delay profile II

References

[1] Cimini, "Analysis and simulation of a digital mobile channel using orthogonal frequency division multiplexing," IEEE Trans. Commun., vol. COMM-33, pp. 665-675, July 1985

[2] Weinstein and Ebert, "Data transmission by frequency-division multiplexing using the discrete Fourier transform," IEEE Trans. Commun., vol. COMM-19, pp. 628-634, Oct. 1971

[3] H. Cheon and D. Hong, "Effect of channel estimation error in OFDM-based WLAN," IEEE Comm. letter, vol. 6, no. 5, May 2002

[4] X. Tang, M. Alouini and A. Goldsmith, "Effect of channel estimation error on M-QAM BER performance in Rayleigh fading," IEEE Trans. on Comm., vol. 47, no. 12, Dec. 1999

[5] R. Negi and J. Cioffi, "Pilot tone selection for channel estimation in a mobile OFDM system," IEEE Trans. on Consumer Electronics, vol. 44, no. 3, Aug. 98